2014 IEEE International Conference on Robotics & Automation (ICRA)
Hong Kong Convention and Exhibition Center
May 31 - June 7, 2014. Hong Kong, China

Contact Dynamics of Massage Compliant Robotic Arm and Its Coupled Stability

Yuancan Huang[1,2], Philippe Souères[2] and Jian Li[1]

Abstract— **In this paper, contact dynamics of robot massage is described by the port-Hamiltonian modelling approach. In order to capture accurately the inherent characteristics of the human body in lumped-parameter manners, the conventional linear Kelvin-Voigt models are replaced by the nonlinear Hunt-Crossley models. As an application of the contact dynamics, coupled stability of compliant robotic arm with impedance control is theoretically analyzed from energetic viewpoints. Experiments are done to verify the massage stability. The proposed contact dynamics evidently has great potential on performance improvement of robot massage, which will be our research subject.**

I. INTRODUCTION

Naturally, robots are chosen to automate massage activities that are world-popular but laborious, repetitive, and time-consuming. In order to guarantee both performance and safety of robot massage, an integrated rotary compliant joint was designed [1], by which a 4-DOF anthropomorphic complaint arm was developed for the traditional Chinese medicine remedial massage [2]. Impedance control and its variants are used by almost all massage robots in the literatures in spite of the criticism on its performance and possible failures [3], [4], for they can guarantee the stable interaction with an unknown environment [5], [6]. However, knowledge on contact dynamics is instrumental in improving the performance of impedance control and exploring its limits [7], [8]. As our best knowledge, there is not yet the relevant works on this aspect for massage robots.

The port-Hamiltonian approach is one of port-based network modeling approaches, which has been recently developed to model complex dynamical systems [9], [10] by defining port variables and delineating interconnection of subsystems by means of the power continuity, which results in the power-conserving Dirac structure [11]. In this paper, the port-Hamiltonian approach is adopted to model the contact dynamics of robot massage. The contribution of our works is threefold: The impedance control in [12], [13] is reformulated from energetic viewpoints, and the coupled stability is reassured in port-Hamiltonian framework; we generate a promising perspective to improve interacted behaviors of impedance control with better knowledge on the contact dynamics of robot massage; new control schemes by port-interconnection, such as IPC [14] and IDA-PBC [15], may be used to regulate robots for massage.

In the remaining, the port-based Hamiltonian modelling approach is briefly introduced in Section II, and contact kinematics is calculated by mathematically describing the surfaces of the body and the massage head in Section III. Then, the interconnection structure of robot massage is introduced, by which the corresponding Dirac structure is derived, and then each component dynamics in this interconnection is described independently with consideration of external ports. In Section V, impedance control is reformulated in full-state feedback form, and coupled stability is analyzed from energetic viewpoints. Some experiments are fulfilled to verify the coupled stability during robot massage in Section VI. Finally, Section VII draws the conclusions and describes a perspective on the further applications of contact dynamics.

II. PORT-HAMILTONIAN MODELLING APPROACH

A. Dirac Structure

Let $\mathscr{F} \times \mathscr{F}^*$ denote the space of power variables, with $\mathscr{F}$ being an n-dimensional linear space, which is the space of flows (*e.g.*, velocities in mechanical domain and currents in electrical domain), and $\mathscr{F}^*$ being its dual, which is the space of efforts (*e.g.*, forces in mechanical domain and voltages in electrical domain), and let the dual product $\langle \boldsymbol{f}, \boldsymbol{e} \rangle$ denote the power associated with the power port $(\boldsymbol{e}, \boldsymbol{f}) \in \mathscr{F} \times \mathscr{F}^*$.

Definition 2.1: A (constant) Dirac structure on $\mathscr{F}$ is a linear subspace $\mathscr{D} \subset \mathscr{F} \times \mathscr{F}^*$ such that $\dim \mathscr{D} = \dim \mathscr{F}$ and $\langle \boldsymbol{f}, \boldsymbol{e} \rangle = 0$, $\forall (\boldsymbol{e}, \boldsymbol{f}) \in \mathscr{D}$.

Remark 2.2: The condition implies that, if each pair $(\boldsymbol{e}, \boldsymbol{f})$ belongs to the Dirac structure, then $\langle \boldsymbol{f}, \boldsymbol{e} \rangle = 0$, *i.e.*, the sum of instantaneous powers passing through the port vanishes. This generalizes the Tellegen's theorem in electrical domain and will lead to a rigorous description of a interconnection structure which can be directly used for dynamical analysis.

B. Port-Hamiltonian System (PHS)

Consider a lumped-parameter physical system defined on a manifold M with local coordinates $\boldsymbol{x} \in \mathbb{R}^n$. The total energy is the Hamiltonian $H(\boldsymbol{x})$. Assume that there is a multibond boundary port with port variable pair $(\boldsymbol{e}_b, \boldsymbol{f}_b) \in \mathbb{R}^m \times \mathbb{R}^m$. For each $\boldsymbol{x} \in M$, we consider $\mathscr{F}_x = T_x M \times \mathbb{R}^m$ and $\mathscr{F}_x^* = T_x^* M \times \mathbb{R}^m$ and define a Dirac structure $\mathscr{D}(\boldsymbol{x}) \subset \mathscr{F}_x \times \mathscr{F}_x^*$. The flow variables of energy-storing elements are given as $\dot{\boldsymbol{x}}(t)$ and its effort variables as $\partial H / \partial \boldsymbol{x}$, which implies that $\langle \partial H / \partial \boldsymbol{x}, \dot{\boldsymbol{x}}(t) \rangle = dH/dt$ is the energy increase. In order to

This work was supported partially by the National Natural Sciences Foundation of China under Research Grant 61075080 and by the French project ROMEO2

[1]Yuancan Huang and Jian Li are with the Institute of Intelligent Robot, School of Mechatronical Engineering, Beijing Institute of Technology, 100081 Beijing, China. yuancanhuang@bit.edu.cn.

[2]Philippe Souères and Yuancan Huang are with Laboratoire d'Architecture et d'Analyse des Système, Centre National de la Recherche Scientifique (LAAS-CNRS), University of Toulouse, 31077 Toulouse, France. Philippe.Soueres@laas.fr.

978-1-4799-3684-7/14/$31.00 ©2014 IEEE

have a consistent sign convention that energy flows from the boundary ports into the system and from the internal network into the energy storing elements, let $\boldsymbol{f}_x = -\dot{\boldsymbol{x}}$ and $\boldsymbol{e}_x = \partial H/\partial \boldsymbol{x}$. Hence, an Implicit Port-Hamiltonian System (IPHS) on M is defined by the set of differential and algebraic equations (DAE):

$$\left(-\dot{\boldsymbol{x}}, \boldsymbol{f}_b, \frac{\partial H}{\partial \boldsymbol{x}}, \boldsymbol{e}_b\right) \in \mathscr{D}(\boldsymbol{x}), \ \forall \boldsymbol{x} \in M$$

with the power-conserving property

$$0 = \langle \boldsymbol{f}, \boldsymbol{e}\rangle = \langle \boldsymbol{f}_x, \boldsymbol{e}_x\rangle + \langle \boldsymbol{f}_b, \boldsymbol{e}_b\rangle = -\frac{\partial H}{\partial \boldsymbol{x}}\dot{\boldsymbol{x}} + \boldsymbol{e}_b^T \boldsymbol{f}_b$$

from which $dH/dt = \boldsymbol{e}_b^T \boldsymbol{f}_b$. By [9], an explicit input/output PHS is given by:

$$\Sigma : \begin{cases} \dot{\boldsymbol{x}} = J(\boldsymbol{x})\frac{\partial H}{\partial \boldsymbol{x}} + g(\boldsymbol{x})\boldsymbol{u}, \\ \boldsymbol{y} = g(\boldsymbol{x})^T \frac{\partial H}{\partial \boldsymbol{x}} + B(\boldsymbol{x})\boldsymbol{u}, \end{cases}$$

where g is arbitrary, J and B are both skew-symmetric, and $\boldsymbol{y} = (\boldsymbol{f}_{b_1}^T,\ \boldsymbol{e}_{b_2}^T)^T$, $\boldsymbol{u} = (\boldsymbol{e}_{b_1}^T,\ \boldsymbol{f}_{b_2}^T)^T$.

III. Contact Kinematics

The body and the massage head are treated as two rigid bodies with smooth, orientable surfaces X_1 and X_2, whose Gauss maps are defined as $\boldsymbol{n}_1$ and $\boldsymbol{n}_2$, respectively. As a result, the contact kinematics is amounted to the motion between two points p_1 and p_2 on the surfaces X_1 and X_2 with the shortest distance. Under convexness assumption, there are always such two unique points p_1 and p_2 in the boundary $X_1 \cup X_2$ whose linking line l_n is normal to both the surfaces X_1 and X_2. Given a point $c \in l_n$ (*e.g.*, the desired contact point), there is a unique plane π orthogonal to l_n and passing through the point c as shown in Fig.1.

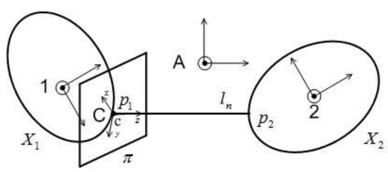

Fig. 1: Two points on X_1 and X_2 with the shortest distance.

Let $\boldsymbol{p}_i,\ i = 1, 2$, denote the position vector of the point p_i in its own frames 1 and 2. A minimum sign distance $\Delta \in \mathbb{R}$ is defined as:

$$\Delta = \langle \boldsymbol{n}_1, T_2^1 \boldsymbol{p}_2 - \boldsymbol{p}_1\rangle,$$

where T_2^1 represents the relative configuration of two frames 1 and 2. When $\Delta > 0$, the bodies are not in contact; when $\Delta = 0$, the bodies are in contact; when $\Delta < 0$, the bodies penetrate each other by a distance of $|\Delta|$. The velocities of p_1 and p_2 are uniquely determined by the following equations [16]:

$$\left[\boldsymbol{n}_{1*} + T_2^1 \boldsymbol{n}_{2*} T_1^2 (I + \Delta \boldsymbol{n}_{1*})\right] \dot{\boldsymbol{p}}_2 = \boldsymbol{t}_2^{1,1} + T_2^1 \boldsymbol{n}_{2*}(\dot{\Delta}\boldsymbol{n}_2 - \boldsymbol{t}_1^{2,2}\boldsymbol{p}_2)$$
$$\left[\boldsymbol{n}_{2*} + T_1^2 \boldsymbol{n}_{1*} T_2^1 (I + \Delta \boldsymbol{n}_{2*})\right] \dot{\boldsymbol{p}}_1 = \boldsymbol{t}_1^{2,2} + T_1^2 \boldsymbol{n}_{1*}(\dot{\Delta}\boldsymbol{n}_1 - \boldsymbol{t}_2^{1,1}\boldsymbol{p}_1),$$

where I is the unit matrix, $\boldsymbol{t}_j^{i,i} = -T_j^i \boldsymbol{t}_i^{j,j} T_i^j$ is a relative twist of the two bodies expressed in frame j, and $\boldsymbol{n}_{i*}$ represents the corresponding tangent map. In addition, $\dot{\Delta} = \langle \boldsymbol{n}_1, \boldsymbol{t}_2^{1,1} T_2^1 \boldsymbol{p}_2\rangle$ and $\Delta > \Delta_{\min}$ for some $\Delta_{\min} < 0$, which depends on properties of the body and the massage head. In our case, since $\dot{\boldsymbol{p}}_2 = 0$, the velocity relations are rewritten as:

$$\left[\boldsymbol{n}_{2*} + T_1^2 \boldsymbol{n}_{1*} T_2^1 (I + \Delta \boldsymbol{n}_{2*})\right] \dot{\boldsymbol{p}}_1 = \boldsymbol{t}_1^{2,2} + T_1^2 \boldsymbol{n}_{1*}(\dot{\Delta}\boldsymbol{n}_1 - \boldsymbol{t}_2^{1,1}\boldsymbol{p}_1),$$
$$\boldsymbol{t}_2^{1,1} + T_2^1 \boldsymbol{n}_{2*}(\dot{\Delta}\boldsymbol{n}_2 - \boldsymbol{t}_1^{2,2}\boldsymbol{p}_2) = 0.$$

IV. Contact Dynamics

A. Port-Based Model of Robot Massage

During massages, one is asked sitting on a chair or lying on a bed, and keeping relaxed and steady as far as possible meanwhile not actively exerting any force back. Therefore, it is rather reasonable that the human body is modeled as an inertial mass with a pair of spatial spring and damper on the upper side and a spatial spring on the lower side, where the pair of spatial spring and damper represents the viscoelasticity of soft tissues, and the spatial spring replicates the reaction force on the robotic arm from the chair or the bed, or by one who tries to keep his body steadily, see Fig. 2.

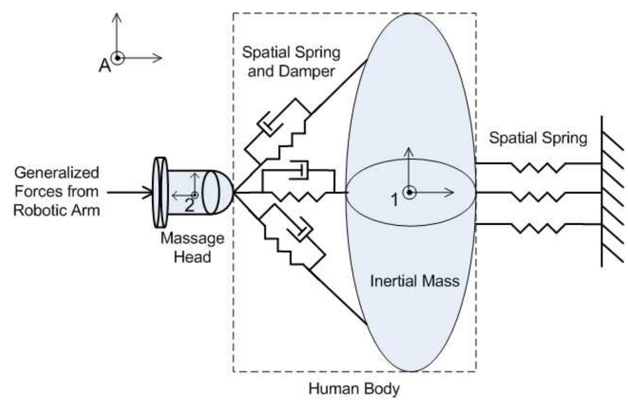

Fig. 2: Port-based model of robot massage.

From the view point of port-based network modelling, a contact Dirac structure interconnects the robotic arm with the inertial mass by a spatial spring representing the body with kinematic constraints, the storage elements representing the elastic effect of soft tissue, and the dissipation elements representing the viscous effect of soft tissue and Coulomb friction. Optionally, one control port can be added to regulate the behaviors of the robotic arm. Figure 3 shows the interconnection structure of port-based model.

B. Mathematical Description of Contact Dirac Structure

Define a binary signal s_Δ as:

$$s_\Delta = \begin{cases} 0, & \text{if } \ \Delta \le 0, \\ 1, & \text{otherwise.} \end{cases}$$

Then, $s_\Delta = 0$ if there is contact and $s_\Delta = 1$ if there is no contact. In practice, the massage head is required to only roll around the normal of the body. Thus its velocity screws $se(3)$ can be decomposed into two terms involving rolling around the normal or not: the screws $(v_x, v_y, v_z, \omega_z)$ representing three translations on the plane π and one pure rotation around

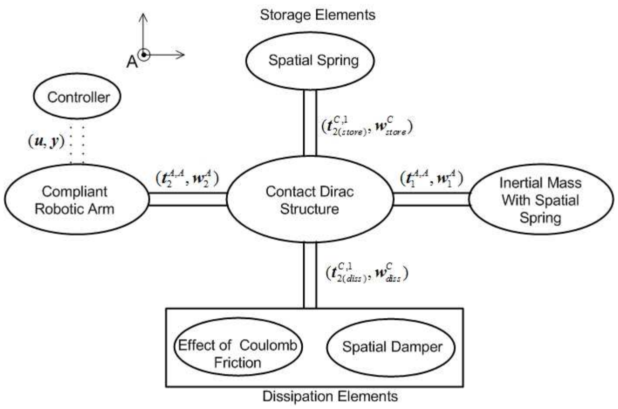

Fig. 3: Interconnection structure of port-based model.

l_n, and the others (ω_x, ω_y) representing two pure rotations around two axis lying on π and passing through c, namely,

$$se(3) = R_{xy} \oplus (se(2) \times T_z),$$

where $R_{xy} := span\{\omega_x, \omega_y\}$ and Lie algebra $se(2) \times T_z$ represents the motions on π together with the normal translation along l_n.

An inertial reference frame A and the contact frame C where origin lies at the contact point c and z axis aligns to l_n are assigned first. Define a projection operator $P_{se(2)\times T_z} : se(3) \to se(2) \times T_z$, which can be represented by the matrix P while coordinate frames are selected. Its adjoint operator $P^*_{se(2)\times T_z}$ maps wrench $\boldsymbol{w}^C_{2,1} \in (se(2) \times T_z)^*$ into wrench $P'\boldsymbol{w}^C_{2,1} \in se^*(3)$ where the prime denotes matrix transpose. In four ports $(\boldsymbol{t}^{A,A}_1, \boldsymbol{w}^A_1)$, $(\boldsymbol{t}^{A,A}_2, \boldsymbol{w}^A_2)$, $(\boldsymbol{t}^{C,1}_{2(store)}, \boldsymbol{w}^C_{store})$ and $(\boldsymbol{t}^{C,1}_{2(diss)}, \boldsymbol{w}^C_{diss})$, there exist the following velocity and force constraints:

$$\begin{aligned}
&\boldsymbol{t}^{C,1}_{2(store)} = \boldsymbol{t}^{C,1}_{2(diss)} = (s_\Delta - 1)P\,\mathrm{Ad}_{T^C_A}\boldsymbol{t}^{A,A}_1 + (1 - s_\Delta)P\,\mathrm{Ad}_{T^C_A}\boldsymbol{t}^{A,A}_2,\\
&\boldsymbol{w}^A_1 = (1 - s_\Delta)\mathrm{Ad}'_{T^C_A} P'\boldsymbol{w}^C_{store} + (1 - s_\Delta)\mathrm{Ad}'_{T^C_A} P'\boldsymbol{w}^C_{diss},\\
&\boldsymbol{w}^A_2 = (s_\Delta - 1)\mathrm{Ad}'_{T^C_A} P'\boldsymbol{w}^C_{store} + (s_\Delta - 1)\mathrm{Ad}'_{T^C_A} P'\boldsymbol{w}^C_{diss},
\end{aligned}$$

where $\mathrm{Ad}_{T^C_A}$ transforms twists from A to C, and its duality $\mathrm{Ad}'_{T^C_A}$ transforms wrenches from A to C. Similar to that in [17], the Dirac structure is written by:

$$E \begin{pmatrix} \boldsymbol{w}^A_1 \\ \boldsymbol{w}^A_2 \\ \boldsymbol{w}^C_{store} \\ \boldsymbol{w}^C_{diss} \end{pmatrix} + F \begin{pmatrix} \boldsymbol{t}^{A,A}_1 \\ \boldsymbol{t}^{A,A}_2 \\ \boldsymbol{t}^{C,1}_{2(store)} \\ \boldsymbol{t}^{C,1}_{2(diss)} \end{pmatrix} = 0 \qquad (1)$$

with

$$E := \begin{pmatrix} I_6 & 0 & (s_\Delta - 1)\mathrm{Ad}'_{T^C_A} P' & (s_\Delta - 1)\mathrm{Ad}'_{T^C_A} P' \\ 0 & I_6 & (1 - s_\Delta)\mathrm{Ad}'_{T^C_A} P' & (1 - s_\Delta)\mathrm{Ad}'_{T^C_A} P' \\ 0 & 0 & 0 & 0 \\ 0 & 0 & 0 & 0 \end{pmatrix}$$

and

$$F := \begin{pmatrix} 0 & 0 & 0 & 0 \\ 0 & 0 & 0 & 0 \\ (s_\Delta - 1)P\,\mathrm{Ad}_{T^C_A} & (1 - s_\Delta)P\,\mathrm{Ad}_{T^C_A} & -I_4 & 0 \\ (s_\Delta - 1)P\,\mathrm{Ad}_{T^C_A} & (1 - s_\Delta)P\,\mathrm{Ad}_{T^C_A} & 0 & -I_4 \end{pmatrix}$$

Here, the switching element s_Δ in E is used to switch off the contact forces $\boldsymbol{w}^C_{store}$ and $\boldsymbol{w}^C_{diss}$ while no contact occurs. The connection of storage and dissipation elements depends on whether contact occurs or not, thus the Dirac structure has variable topology.

C. Hamilton Equations of Compliant Robotic Arm and the Human Body

1) Compliant Robotic Arm: Consider an n-link robotic arm with fully revolute compliant joints where a serial elastic unit is put in connecting the motor shaft with the link in each joint. Assume that the rotor/gear inertia is symmetric around the rotor's axis and that the rotor has no translational motion itself. It has been shown that [18], the total kinetic energy consists of two components: the kinetic energy of the rigid robotic arm where the serial elasticity in joints is neglected, and the rotational kinetic energy of the joint rotors

$$T(\boldsymbol{q}_q, \boldsymbol{q}_\theta, \dot{\boldsymbol{q}}_q, \dot{\boldsymbol{q}}_\theta) = \frac{1}{2}\dot{\boldsymbol{q}}'_q M(\boldsymbol{q}_q)\boldsymbol{q}_q + \frac{1}{2}\dot{\boldsymbol{q}}'_\theta B \boldsymbol{q}_\theta, \qquad (2)$$

where $\boldsymbol{q}_q = (q_1, \ldots, q_n)'$ and $\boldsymbol{q}_\theta = (\theta_1, \ldots, \theta_n)'$ be the generalized coordinates where q_i and θ_i represent the angular positions of link i and rotor i respectively, $M(\boldsymbol{q}_q)$ is the inertia matrix of the rigid robotic arm calculating by standard techniques once the rotor masses are regarded as a part of the proximal links for their inertia tensor, and B the inertia matrix of the rotors.

The elastic potential of the serial elastic unit is

$$P(\boldsymbol{q}_q, \boldsymbol{q}_\theta) = \frac{1}{2}(\boldsymbol{q}_\theta - \boldsymbol{q}_q)' K (\boldsymbol{q}_\theta - \boldsymbol{q}_q),$$

where K is a diagonal matrix with stiffness coefficients as its diagonal elements. Invoking again the symmetry assumption, the gravitational potential is a function only of $\boldsymbol{q}_q$. Therefore, the total potential energy is written as:

$$U(\boldsymbol{q}_q, \boldsymbol{q}_\theta) = P(\boldsymbol{q}_q, \boldsymbol{q}_\theta) - G(\boldsymbol{q}_q), \qquad (3)$$

where the gravitational potential energy term $G(\boldsymbol{q}_q)$ is found from the standard formulae for rigid robots. Hence, the Lagrangian is

$$L(\boldsymbol{q}_q, \boldsymbol{q}_\theta, \dot{\boldsymbol{q}}_q, \dot{\boldsymbol{q}}_\theta) = T(\boldsymbol{q}_q, \boldsymbol{q}_\theta, \dot{\boldsymbol{q}}_q, \dot{\boldsymbol{q}}_\theta) - U(\boldsymbol{q}_q, \boldsymbol{q}_\theta).$$

By the Legendre transform of $L(\boldsymbol{q}_q, \boldsymbol{q}_\theta, \dot{\boldsymbol{q}}_q, \dot{\boldsymbol{q}}_\theta)$, the corresponding Hamiltonian function is

$$\begin{aligned}
H_{robot}(\boldsymbol{q}_q, \boldsymbol{q}_\theta, \boldsymbol{p}_q, \boldsymbol{p}_\theta) &= \frac{1}{2}\boldsymbol{p}'_q M^{-1}(\boldsymbol{q}_q)\boldsymbol{p}_q + \frac{1}{2}\boldsymbol{p}'_\theta B^{-1}\boldsymbol{p}_\theta \\
&\quad - \frac{1}{2}(\boldsymbol{q}_\theta - \boldsymbol{q}_q)' K (\boldsymbol{q}_\theta - \boldsymbol{q}_q) + G(\boldsymbol{q}_q),
\end{aligned}$$

where $\boldsymbol{p}_q = \partial L / \partial \dot{\boldsymbol{q}}_q$ and $\boldsymbol{p}_\theta = \partial L / \partial \dot{\boldsymbol{q}}_\theta$. Assume that $\boldsymbol{t}^{A,A}_2 = J_R(\boldsymbol{q}_q)\dot{\boldsymbol{q}}_q$ where $J_R(\boldsymbol{q}_q)$ is the Jacobian. Its dual relation is $\tau_{ext} = J'_R(\boldsymbol{q}_q)\boldsymbol{w}^A_2$ where τ_{ext} represents the external torque acting on the robotic arm. If one control port $(\boldsymbol{u},\boldsymbol{y})$ and one interacted port $(\boldsymbol{t}_2^{A,A},\boldsymbol{w}_2^A)$ are added, a port-Hamiltonian system with two ports is written by:

$$\begin{pmatrix} \dot{\boldsymbol{p}}_q \\ \dot{\boldsymbol{p}}_\theta \\ \dot{\boldsymbol{q}}_q \\ \dot{\boldsymbol{q}}_\theta \end{pmatrix} = \begin{pmatrix} 0 & 0 & -I_q & 0 \\ 0 & 0 & 0 & -I_\theta \\ I_q & 0 & 0 & 0 \\ 0 & I_\theta & 0 & 0 \end{pmatrix} \times \tag{4}$$

$$\begin{pmatrix} M^{-1}(\boldsymbol{q}_q)\boldsymbol{p}_q \\ B^{-1}\boldsymbol{p}_\theta \\ \frac{1}{2}\boldsymbol{p}_q^T \frac{\partial M^{-1}(\boldsymbol{q}_q)}{\partial \boldsymbol{q}_q}\boldsymbol{p}_q - K(\boldsymbol{q}_\theta - \boldsymbol{q}_q) + \boldsymbol{g}(\boldsymbol{q}_q) \\ K(\boldsymbol{q}_\theta - \boldsymbol{q}_q) \end{pmatrix} + \begin{pmatrix} 0 \\ 0 \\ J_R'(\boldsymbol{q}_q)\boldsymbol{w}_2^A \\ \boldsymbol{u} \end{pmatrix},$$

$$\boldsymbol{t}_2^{A,A} = J_R(\boldsymbol{q}_q)\dot{\boldsymbol{q}}_q,$$

where $\boldsymbol{u}$ is the control torque and $\boldsymbol{g}(\boldsymbol{q}_q) = \partial G(\boldsymbol{q}_q)/\partial \boldsymbol{q}_q$.

2) The Human Body: Here, the body is modeled as a combination of an inertial mass with inertia matrix $M_I(\boldsymbol{q}_I)$, where $\boldsymbol{q}_I$ is the configuration vector of the body, and a linear spatial spring with the stiffness matrix $K_I(\boldsymbol{q}_I)$. The Hamiltonian of the body can be written as:

$$H_{body}(\boldsymbol{p}_I,\boldsymbol{q}_I) = \frac{1}{2}\boldsymbol{p}_I' M_I^{-1}(\boldsymbol{q}_I)\boldsymbol{p}_I - \frac{1}{2}(\boldsymbol{q}_I - \boldsymbol{q}_I^0)' K_I(\boldsymbol{q}_I)(\boldsymbol{q}_I - \boldsymbol{q}_I^0),$$

where $\boldsymbol{q}_I^0$ is some reference position of the body. The port-Hamiltonian equation with the port pair $(\boldsymbol{t}_1^{A,A},\boldsymbol{w}_1^A)$ is

$$\begin{aligned} \dot{\boldsymbol{q}}_I &= M_I^{-1}(\boldsymbol{q}_I)\boldsymbol{p}_I + J_I^+(\boldsymbol{q}_I)\boldsymbol{t}_1^{A,A}, \\ \dot{\boldsymbol{p}}_I &= -\frac{1}{2}\boldsymbol{p}_I' \frac{\partial M^{-1}(\boldsymbol{q}_I)}{\partial \boldsymbol{q}_I}\boldsymbol{p}_I + K_I(\boldsymbol{q}_I)(\boldsymbol{q}_I - \boldsymbol{q}_I^0) \\ &\quad + \frac{1}{2}(\boldsymbol{q}_I - \boldsymbol{q}_I^0)' \frac{\partial K_I(\boldsymbol{q}_I)}{\partial_{\boldsymbol{q}_I}}(\boldsymbol{q}_I - \boldsymbol{q}_I^0), \\ K_I(\boldsymbol{q}_I)(\boldsymbol{q}_I^0 - \boldsymbol{q}_I) &= J_I'(\boldsymbol{q}_I)\boldsymbol{w}_1^A, \end{aligned} \tag{5}$$

where $J_I^+(\boldsymbol{q}_I)$ is the psuedoinverse of the Jacobian from the inertial frame A to the frame 1. Since both kinetic energy and elastic potential are conserved, the energy balancing relation is $dH_I/dt = -(\boldsymbol{w}_1^A)'\boldsymbol{t}_1^{A,A}$. Of course, this model can be simplified according to practical requirements, *e.g.*, it degenerates into the kinematics constraints if no dynamics is considered, or the inertia matrix $M_I(\boldsymbol{q}_I)$ and/or the stiffness matrix $K_I(\boldsymbol{q}_I)$ are constant.

D. Viscoelasticity of the Body and Coulomb Friction

1) Hunt-Crossley Model: The simple model characterizing soft tissues of the body is known as the Kelvin-Voigt model, which is represented by the parallel of a linear spring and a viscous damper. However, the linear model is not suitable to describe the behavior of human tissues, where viscous effects are substantial [19], [7]. Hunt and Crossley [20] showed that it is possible to obtain a behavior that is in better agreement with the physical intuition if the damping coefficient is made dependent on the body's relative penetration. If $F(t)$ is the force exerted by the soft tissue on the massage head during contact, the nonlinear model is expressed as:

$$F(t) = \begin{cases} k \mid \Delta(t) \mid^n + \lambda \mid \Delta(t) \mid^n \dot{\Delta}(t), & \Delta \le 0 \\ 0, & \Delta > 0 \end{cases}$$

where the exponent n is usually close to unity. Since the contact surface increases as the penetration depth increases, the exponent allows taking into account the stiffness variation due to a larger contact area. For the sake of simplicity, let $n = 1$, *i.e.*, assume that the contact area does changes with respect to the penetration depth. It is important to note that the physical consistency of the model can be preserved by a proper generalization to the full geometrical contact description (more than one DOF), as discussed in [21], [17]. Thus a spatial spring in parallel with a spatial damper is used to describe the viscoelasticity of the body.

2) Viscoelastic of the Body: The massage head, which is much harder than soft tissues in the body, may be regarded as a rigid body. The contact frame C is defined as follows: the contact point c is the massage point on the body, the plane π coincides with the tangent plane at c, and the line l_n connects the contact point c with the massage head. According to the Hunt-Crossley model with $n = 1$, there is [22]

$$\boldsymbol{w}_{store}^C = K_B \delta \boldsymbol{t}_{2(store)}^{C,1}, \quad \boldsymbol{w}_{diss(B)}^C = D_B\left(\delta \boldsymbol{t}_{2(store)}^{C,1}\right)\boldsymbol{t}_{2(store)}^{C,1},$$

where $\delta \boldsymbol{t}_{2(store)}^{C,1}$ represents the variation of the twist $\boldsymbol{t}_{2(store)}^{c,1}$, K_s is a two-covariant stiffness tensor such that $K_s \delta \boldsymbol{t}$ is the restoring force resulting from the deformation $\delta \boldsymbol{t}$ around the equilibriums, and $D_B\left(\delta \boldsymbol{t}_{2(store)}^{C,1}\right)$ is the damping matrix which locally is defined as $\left(\delta \boldsymbol{t}_{2(store)}^{C,1}\right)' D$ with a constant diagonal matrix D. The stiffness tensor K_s can be defined globally by using a connection [23] and then the potential function P_B is constructed from K_s at the minimum by integration of the forces [14]. Furthermore, we can directly define a Rayleigh dissipation function R_B such that $\boldsymbol{w}_{diss(B)}^C = \partial R_B / \partial \boldsymbol{t}_{2(store)}^{C,1}$.

3) Coulomb Friction: In order to consider the effect of friction, a resistive port pair $\left(\boldsymbol{t}_{2(store)}^{C,1}, \boldsymbol{w}_{diss(F)}^C\right)$ is supplemented. The friction force is calculated by $\boldsymbol{w}_{diss(F)}^C = K_f\left(\boldsymbol{t}_{2(store)}^{C,1}\right)\left(\boldsymbol{w}_{diss(B)}^C + \boldsymbol{w}_{store}^C\right)$, where K_f is the sign friction coefficient matrix such that the friction force satisfies velocity reversal conditions. In addition, we have $\boldsymbol{w}_{diss}^C = \boldsymbol{w}_{diss(B)}^C + \boldsymbol{w}_{diss(F)}^C$.

V. Impedance Control and Coupled Stability

A. Impedance Control

In terms of energy shaping viewpoints, an impedance controller with two feedback loops is constructed in [12], [13]. Rewritten in the matrix form, the torque inner loop is

$$\boldsymbol{u} = BB_a^{-1}\boldsymbol{v} + (I - BB_a^{-1})\tau_{meas}, \tag{6}$$

where $\boldsymbol{v}$ is an intermediate control input vector, B_a the motor apparent inertia vector with respect to $\boldsymbol{v}$, and $\boldsymbol{u}$ is the motor torque vector. The impedance outer loop is a PD controller with gravity compensation:

$$\boldsymbol{v} = -K_q(\boldsymbol{q}_q - \boldsymbol{q}_q^d) - D_q\dot{\boldsymbol{q}}_q + \boldsymbol{g}(\boldsymbol{q}_q), \tag{7}$$

where $\boldsymbol{q}_q^d$ is the desired rotor angular position vector, and K_q and D_q are the desired stiffness and damping matrices, respectively. The given impedance control is actually a full-state feedback controller.

However, we cannot derive the expected passivity from the control law (7). A solution is to choose $\boldsymbol{v}$ as a function of only $\boldsymbol{q}_\theta$ and its derivative $\dot{\boldsymbol{q}}_\theta$ by replacing $\boldsymbol{q}_q$ with its stationary equivalent $\hat{\boldsymbol{q}}_q(\boldsymbol{q}_\theta)$, which can be solved in a sufficiently small neighborhood of the equilibrium point from

$$\boldsymbol{q}_\theta = \boldsymbol{f}(\boldsymbol{q}_q) = \boldsymbol{q}_q + K^{-1}[-K_q(\boldsymbol{q}_q - \boldsymbol{q}_\theta) + \boldsymbol{g}(\boldsymbol{q}_q)].$$

Generally, the inverse function $\boldsymbol{f}^{-1}$ has not analytic expression. For a given $\boldsymbol{q}_\theta$, it is possible to approximate the value $\hat{\boldsymbol{q}}_q(\boldsymbol{q}_\theta) = \boldsymbol{f}^{-1}(\boldsymbol{q}_\theta)$ with arbitrary precision by iteration method. The updated control law is written as:

$$\boldsymbol{v} = -K_q\left(\hat{\boldsymbol{q}}_q(\boldsymbol{q}_\theta) - \boldsymbol{q}_q^d\right) - D_q\dot{\boldsymbol{q}}_\theta + \boldsymbol{g}\left(\hat{\boldsymbol{q}}_q(\boldsymbol{q}_\theta)\right), \qquad (8)$$

After this substitution, due to gravity compensation and energy shaping, the Hamiltonian of the overall closed-loop system is given by:

$$H_{close}(\boldsymbol{q}_q, \boldsymbol{q}_\theta, \boldsymbol{p}_q, \boldsymbol{p}_\theta) = \frac{1}{2}\boldsymbol{p}_q' M^{-1}(\boldsymbol{q}_q)\boldsymbol{p}_q + \frac{1}{2}\boldsymbol{p}_\theta' B_a^{-1}\boldsymbol{p}_\theta$$
$$-\frac{1}{2}(\boldsymbol{q}_q - \boldsymbol{q}_\theta)' K(\boldsymbol{q}_q - \boldsymbol{q}_\theta).$$

It has been shown [12], [13] that, for the robots only with rotational joints, there is

$$\frac{dH_{close}}{dt} = -\dot{\boldsymbol{q}}_\theta^T D_q \dot{\boldsymbol{q}}_\theta - (\boldsymbol{w}_2^A)' \boldsymbol{t}_2^{A,A} < -(\boldsymbol{w}_2^A)' \boldsymbol{t}_2^{A,A},$$

i.e., the overall closed system is strictly passive with respect to the port pair $(\boldsymbol{t}_2^{A,A}, -\boldsymbol{w}_2^A)$.

B. Coupled Stability

Putting two dynamical equations (5) and (6) together and combining with the algebraic constraints (1) in which the unknown wrenches and the unknown twists are calculated in terms of the acquired measurements, *e.g.*, $\boldsymbol{t}_{2(store)}^{c,1}$, we obtain the overall contact dynamics of massage compliant robotic arm. Its Hamiltonian is $H = H_{close} + H_{body}$. According to the energy balance relation, we derive

$$\frac{dH}{dt} < \left(\boldsymbol{w}_{diss}^C + \boldsymbol{w}_{store}^C\right)' \boldsymbol{t}_{2(store)}^{C,1} < 0, \qquad \forall s_\Delta \in \{0, 1\}.$$

In other words, the compliant robotic arm with impedance controller is asympotically stable, no matter whether it is in contact with the body or not.

VI. Experimental Verification

To verify the coupled stability, pressing, kneading, and plucking are realized on the human body by the 4-DOF anthropomorphic compliant robotic arm [2] in two scenarios where the subject is sitting on a chair and lying on a bed, see Fig. 4. In robotic language, pressing is an up and down cyclic motion perpendicular to the body; kneading and plucking are, respectively, the circular and rectilinear cyclic motions tangential to the body. In the experiments, all of these massage movements exerts vertically a downward force on the body. During robot massages, force curves are measured by JR3 6DOF force-torque sensors 50M31. The

(a) Lying scenario

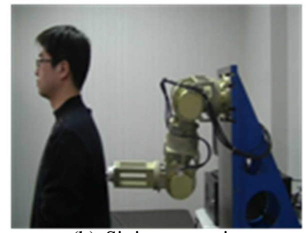

(b) Sitting scenario

Fig. 4: Two scenarios for verifying coupled stability

results in Fig. 5 and Fig. 6 show that the coupled stability is guaranteed in the different massage scenarios, which has been already predicted by the foregoing theoretical analysis.

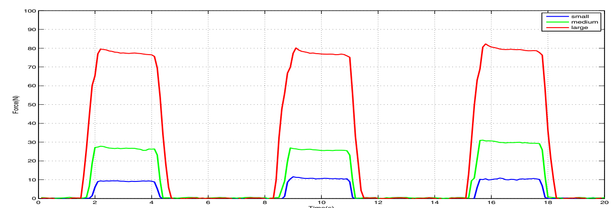

(a) Pressing

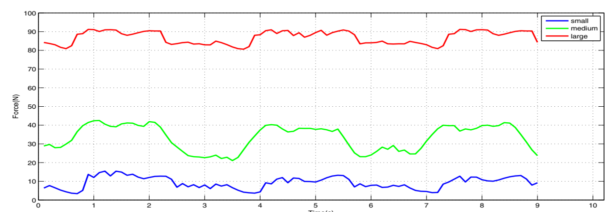

(b) Kneading

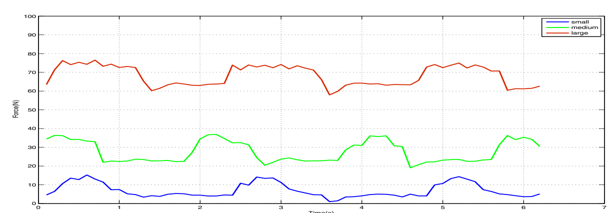

(c) Plucking

Fig. 5: Force curves of robot massage manipulation in lying scenario

VII. Conclusions and Discussions

In this paper, the port-Hamiltonian modelling approach is used to model the massage manipulation by compliant robotic arm. Its usages substantiate three aspects: First, the impedance control for compliant robotic arm in [12], [13] is reformulated from the energetic viewpoints, and coupled stability is reassured in the port-Hamiltonian framework. Second, it is possible to improve the interacted behavior of impedance control with better knowledge on the contact dynamics for massage manipulation. Finally, the control

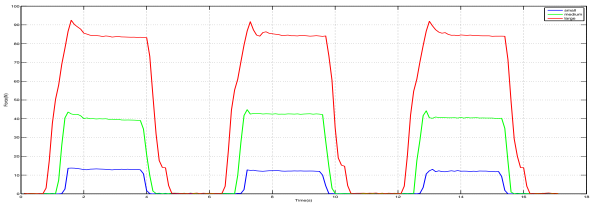

(a) Pressing

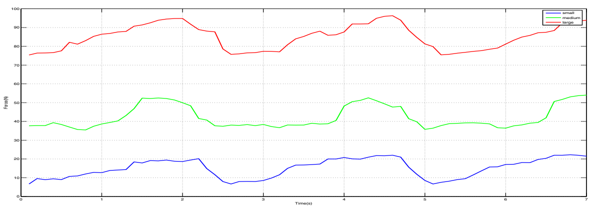

(b) Kneading

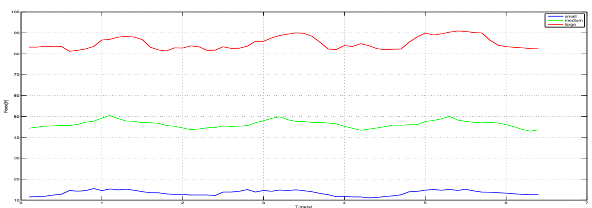

(c) Plucking

Fig. 6: Force curves of robot massage manipulation in sitting scenario

schemes by port-interconnection, which have been intensively studied in the literature, may be used for massage manipulation. Then, pressing, kneading, and plucking are realized on the human body by the 4-DOF anthropomorphic compliant robotic arm in two scenarios to verify the coupled stability during massage manipulation. The results show that coupled stability is guaranteed in the different massage scenarios, as indicated in the theoretical analysis.

In the future, we will use the contact dynamics to study the massage performance of impedance control, to explore the influence of the impedance variation on the body, and to develop new control schemes and new dynamical model so that more complicated massage manipulation is realized, *e.g.*, rolling on the body in which nonholonomic constraints must be considered, and tapping on the body in which we need to capture impact dynamics.

VIII. Acknowledgments

The authors gratefully appreciate the support of this research by the National Natural Sciences Foundation of China. This work was also partially supported by the French project ROMEO2.

References

[1] Y. Huang and *et al.*, “Integrated rotary compliant joint and its impedance-based controller for single-joint pressing massage robot,” in *Proc. of IEEE Int. Conf. on Robotics and Biomimetics*, Guangzhou, China, 2012, pp. 1962–1967.

[2] ——, “Design and control of anthropomorphic BIT soft arms for TCM remedial massage,” in *Proc. of IEEE/RSJ Int. Conf. on Intelligent Robots and Systems*, Tokyo, 2013.

[3] T. Valency and M. Zacksenhouse, “Accuracy/robustness dilemma in impedance control,” *ASME J. Dynam. Syst. Meas. Contr.*, vol. 125, pp. 310–319, 2003.

[4] B. S. S. Chiaverini and L. Villani, “A survey of robot interaction control schemes with experimental comparison,” *IEEE/ASME Trans. on Mechatronics*, vol. 4, no. 3, pp. 273–285, 1999.

[5] N. Hogan, “On the stability of manipulators performing contact tasks,” *IEEE J. Robot. Autom.*, vol. 4, no. 6, pp. 677–686, 1988.

[6] J. E. Colgate and N. Hogan, “Robust control of dynamically interacting systems,” *Int. J. Control*, vol. 48, p. 6588, 1988.

[7] C. M. N. Diolaiti and S. Stramigioli, “Contact impedance estimation for robotic systems,” *IEEE Trans. Robotics*, vol. 21, pp. 925–935, 2005.

[8] S. P. Buerger and N. Hogan, “Complementary stability and loop shaping for improved humanrobot interaction,” *IEEE Trans. Robotics*, vol. 23, pp. 232–244, 2007.

[9] S. S. V. Duindam, A. Macchelli and H. B. (Eds.), *Modeling and Control of Complex Physical Systems-The Port-Hamiltonian Approach*. Berlin: Springer-Verlag, 2009.

[10] A. J. van der Schaft, *L_2-Gain and Passivity Techniques in Nonlinear Control (Communication and Control Engineering Series)*. Berlin, Germany: Springer-Verlag, 2000.

[11] M. Dalsmo and A. J. van der Schaft, “On representation and integrability of mathematical structures in energy-conserving physical systems,” *SIAM J. Control Optim.*, vol. 37, p. 5491, 1999.

[12] C. O. A. Albu-Schäffer and G. Hirzinger, “A unified passivity-based control framework for position, torque and impedance control of flexible joint,” *Int. J. Robot. Res.*, vol. 26, no. 1, pp. 23–39, 2007.

[13] A. K. C. Ott, A. Albu-Schäffer and G. Hirzinger, “On the passivity-based impedance control of flexible joint robots,” *IEEE J. Robotics Auromat.*, vol. 24, no. 2, pp. 416–429, 2008.

[14] S. Stramigioli, *Modeling and IPC Control of Interactive Mechanical Systems: A Coordinate Free Approach*. London, U.K.: Springer-Verlag, 2001.

[15] A. A. J. Acosta, R. Ortega and A. D. Mahindrakar, “Interconnection and damping assignment passivity-based control of mechanical systems with underactuation degree one,” *IEEE Trans. on Automatic Control*, vol. 50, no. 12, pp. 1936–1955, 2005.

[16] V. Duindam and S. Stramigioli, “Modeling the kinematics and dynamics of compliant contact,” in *Proc. of the 2003 IEEE International Conference on Robotics and Automation*, Taipei, Taiwan, 2003, pp. 4029–4034.

[17] S. Stramigioli and V. Duindam, “Port based modeling of spatial viscoelastic contacts,” *Eur. J. Control*, vol. 10, p. 510519, 2004.

[18] M. W. Spong, “Modeling and control of elastic joint robots,” *ASME J. Dynam. Syst. Meas. Contr.*, vol. 109, no. 4, pp. 310–319, 1987.

[19] G. Gilardi and I. Sharf, “Literature survey of contact dynamics modeling,” *J. Mech. Mach. Theory*, vol. 37, no. 10, p. 12131239, 2002.

[20] K. Hunt and F. Crossley, “Coefficient of restitution inierpreted as damping in vibroimpact,” *ASME J. Appl. Mech.*, vol. 42, p. 440445, 1975.

[21] S. Stramigioli, “Modeling the kinematics and dynamics of compliant contact,” in *Proc. 2nd Workshop Lagrangian, Hamiltonian Methods Nonlinear Control*, Sevilla, Spain, 2003, p. 1726.

[22] L. V. F. Ficuciello, R. Carloni and S. Stramigioli, “Port-hamiltonian modeling for soft-finger manipulation,” in *Proc. of the 2010 IEEE international conference on Intelligent Robots and Systems*, Taipei, 2010, pp. 4281–4286.

[23] M. Zefran and V. Kumar, “Affine connections for the cartesian stiffness matrix,” in *Proc. of the 1997 IEEE international conference on robotics and automation*, New Mexico, 1997, pp. 1376–1381.